Techno-economic Analysis of Integrated Processes for the Treatment and Valorization of Coal Mine Effluents

M. Micari[1*], A. Cipollina[2], A. Tamburini[2*], M. Moser[1], V. Bertsch[1,3], G. Micale[2]

[1] German Aerospace Center (DLR), Institute of Engineering Thermodynamics, Pfaffenwaldring 38-40, 70569 Stuttgart, Germany

[2] Dipartimento di Ingegneria (DI), Università degli Studi di Palermo (UNIPA), viale delle Scienze Ed. 6, 90128 Palermo, Italy

[3] Ruhr-Universität Bochum, Chair of Energy Systems and Energy Economics, Universitätsstr. 150, 44801 Bochum, Germany

*corresponding authors: Marina.Micari@dlr.de, alessandro.tamburini@unipa.it

ABSTRACT

The disposal of highly concentrated coal mine effluents into the environment constitutes a severe threat to the natural ecosystem. This work proposes and compares five novel treatment chains to purify the effluent and recover raw materials. The chains present different combinations of pre-treatment and concentration technologies. In all cases, the solution sent to the concentration step is concentrated up to saturation to recover water and sodium chloride.

Concerning the technical performances, the treatment chains are compared in terms of total energy demand and salt recovery. Furthermore, the economic feasibility assessment is performed via a novel global parameter, i.e. the levelized cost of the produced NaCl crystals (Levelized Salt Cost, LSC).

The energetic and economic analysis of the chains highlighted that the thermal energy demand of the concentration technology covers the highest share of the total demand and the relevant costs are among the highest expenditures. Also, the revenues given by $Mg(OH)_2$ production were found to play a key role in offsetting the treatment costs. Among the treatment chains analyzed, the one composed by two nanofiltration units and three crystallizers in the pre-treatment step and a multi-effect distillation unit in the concentration step showed the highest recovery of NaCl and turned out to be the most economically feasible. The relevant LSC (~90 $/ton_{NaCl}$) was the lowest and it was comparable with the lower bound of the current range of price of high-purity NaCl crystals.

In conclusion, the findings of this work contribute to improving the sustainability of the coal mine industrial sector, by proposing economically feasible solutions for the treatment and valorization of its polluted effluent.

KEYWORDS

Coal mine effluent; Wastewater treatment; Techno-economic analysis; Economic feasibility; Resource recovery; Energy demand

1. INTRODUCTION

Coal extraction is realized through opencast or underground methods and both strongly affect the environment because of the discharge of significant volumes of wastewater (Tiwary 2001). Coal mine wastewater may assume a wide range of physicochemical properties and pH, depending on the hydrogeology of the mine responsible for its discharge (Masindi et al. 2018).

Firstly, coal mines produce significant amounts of acid effluents, often referred to as Acid Mine Drainage (AMD). These effluents would cause severe problems to human health and environment, if discharged. The acidity of the solutions depends on the content of pyrite (FeS_2) in the coal and their release into the environment would lead to deterioration of the quality of the receiving water and damage of natural ecosystems (Baruah and Khare 2010). Moreover, AMD typically presents metal ions, such as iron, copper, aluminium, nickel, whose solubility increases at low pH up to toxic levels (Akcil and Koldas 2006). For this reason, several studies have focused on the development of processes to neutralize the discharged solution: among these, the active mine treatment is one of the most commonly used method (Qin et al. 2019). This process consists in mixing the effluent with alkaline solutions in order to increase the pH and to let the metal ions precipitate in the form of hydroxides (Kalin et al. 2006). Alternative methods include the employment of wetlands where the neutralization occurs via microbial communities (Tarutis et al. 1999) and the in-situ bioremediation through the addition of bacteria to stimulate oxidation and sulphate reduction processes (Christensen et al. 1996, Gibert et al. 2002). In this context, bioremediation systems were tested to assess the feasibility of using the treated water for irrigation. Some of the analysed systems were found to be effective in sulphate removal and economically advantageous (Martins et al. 2010).

Other possible methods to treat AMD include ion-exchange and adsorption (Feng et al. 2000, Motsi et al. 2009, Kefeni et al. 2017a). The selection of the treatment method has been often made by taking into consideration only the technical and the economic factors. However, recent studies focused more on the environmental impact of the remediation systems by performing Life Cycle Assessment analyses (Martínez et al. 2019). In this regard, the environmental impact of the metal-rich sludge generated by the active treatment of AMD was assessed and valorisation strategies were proposed to recover metals and to reduce the waste production (Macías et al. 2017).

In addition, other valuable materials may be recovered from the effluents via the implementation of suitable valorisation strategies. Among the resources that have been mostly recovered, there are ferrite, ferric hydroxide, gypsum, sulphuric acid and rare earth elements (Kefeni et al. 2017b). Various treatment strategies have been proposed: neutralization coupled with reaction steps to produce gypsum ($CaSO_4$) and limestone ($CaCO_3$) (Masindi et al. 2018) or nanofiltration to recover rare earth elements (López et al. 2019). Moreover, Nleya et al. assessed the technical and economic feasibility of applying wastewater treatment technologies to recover sulphuric acid (Nleya et al. 2016).

Furthermore, coal mines produce neutral effluents, characterised by high hardness and high Total Dissolved Solids (TDS). In Poland, a very high amount of chlorides and sulphates were daily discharged into the rivers because of the release of coal mine effluents (Ericsson and Hallmans 1996). This caused severe ecological problems, thus novel treatment strategies were proposed to reduce the waste and recover valuable materials, in particular gypsum and NaCl crystals (Turek et al. 2005a). The first treatment plant proposed by Ericsson et al. for the

effluents of two coal mines in Poland was constituted by a pre-treatment step, two concentration steps (reverse osmosis and a thermal desalination process) and crystallization of sodium chloride. In this plant, the highest share of energy consumption was due to the vapour compressors in the thermal concentration step (Ericsson and Hallmans 1996). Then, Turek et al. proposed a treatment process to achieve a zero liquid discharge utilization of the effluent discharged by another polish coal mine (Turek et al. 2005a). In this case, two treatment trains with different pre-treatment and pre-concentration steps were devised for highly concentrated and poorly concentrated water: for the first, they proposed the combination of nanofiltration and evaporation, whereas for the second an electrodialysis step was employed. Then, the two permeates that presented a low concentration of bivalent ions were further concentrated and sent to the NaCl crystallizer. Moreover, the same authors demonstrated that using nanofiltration as pre-treatment step allowed for increasing the energetic efficiency of the treatment plant, by reducing the energy consumption of the NaCl crystallizer (Turek et al. 2008). Another work suggested using Vacuum Membrane Distillation to treat a coal mine effluent with high TDS, containing iron and aluminium together with calcium and magnesium (Sivakumar et al. 2013). The obtained permeate resulted to be able to meet the quality standards for potable water, since most of the ions (>95%) was removed during the treatment. Overall, the concern about the release of coal mine effluents into the environment is leading to the development of circular strategies, aimed at reducing the production of waste and at recovering valuable materials. Thus, cleaner production strategies to reduce the waste emissions in coal mines have been proposed in the literature (Dharmappa et al. 2000). However, a very few works have been devoted to presenting novel waste treatment and materials recovery strategies applicable to neutral coal mine effluents and so far, a comprehensive techno-economic comparison of different circular strategies is still missing.

The aim of this work is to perform a comprehensive investigation of different possible treatment chains, devised to recover valuable materials from a coal mine effluent and to reduce the amount of produced waste to be disposed. The case study makes reference to a real coal mine effluent produced in Poland, which presents high TDS, hardness and sulphate concentration. All of the proposed chains make reference to the general treatment scheme reported in Figure 1. This includes a pre-treatment step, composed by Nanofiltration (NF) and crystallization units, for recovering bivalent ions as Mg^{2+} and Ca^{2+}. The pre-treatment phase is followed by a concentration step, which can be completely thermal or given by the combination of thermal and electric membrane processes. In particular, two different configurations were investigated: the concentration step was either based on Multi-Effect Distillation (MED) only or given by the combination of Reverse Osmosis (RO) and direct contact Membrane Distillation (MD). Finally, an end-crystallization step is adopted in all chains to produce sodium chloride crystals.
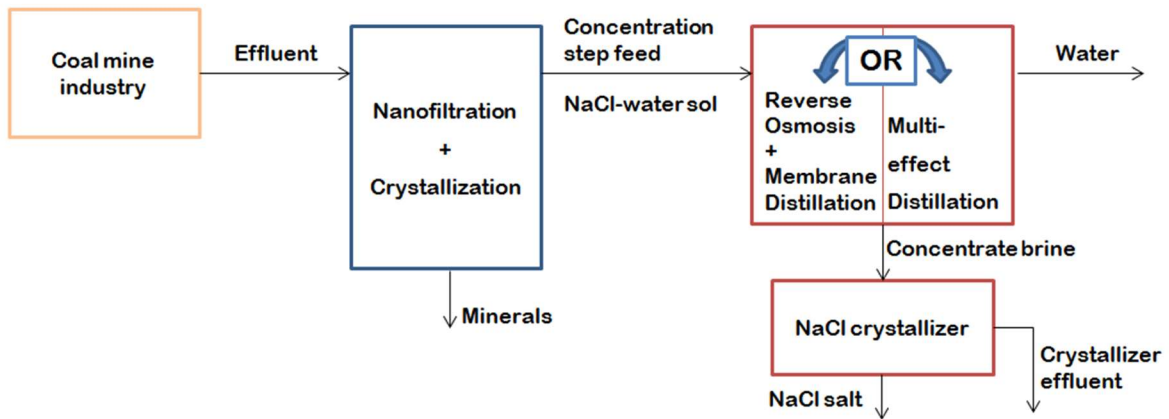
Figure 1. Schematic representation of the treatment process proposed for coal mine effluents.

Five chains are proposed and analysed in details from the energetic and the economic point of view, looking at the energy demands of the single processes, the relevant annualized capital and operating costs and the revenues coming from the recovered by-products. For each system, the economic feasibility is assessed via the calculation of a novel parameter: the levelized cost of the main product of the chain, i.e. the sodium chloride crystals (here defined as Levelized Salt Cost, LSC in [$/ton]). In addition, the chains are compared in terms of the total energy requirements, the levelized cost of the salt and the recovery of salt with respect to the inlet amount.

Overall, this work aims at the identification of the most feasible and less energy-intensive process to treat a very harmful industrial effluent and to recover the valuable materials that it contains.

2. MATERIALS AND METHODS

This section includes three paragraphs. The first shortly presents the methodological approach employed in the present work (Micari et al. 2020). The second describes the five treatment chains devised to purify the coal mine effluent and to recover minerals, water and salt. Finally, the third paragraph reports the definitions of the global outputs used to compare the chains.

2.1 Methodological approach

The methodological approach employed to develop, analyse and compare treatment chains for coal mine effluents has been extensively described in a previous work (Micari et al. 2020). This method is very flexible and applicable to different case studies, when a number of integrated systems have to be developed and compared.

The methodology consists of four inter-related steps:
(a) implementation of techno-economic models of treatment technologies;
(b) definition of inputs and outputs of the models;
(c) development of treatment chains (i.e. how the technologies are interconnected);
(d) comparison through global outputs.

For the treatment chains developed in the present work, we considered nanofiltration and crystallization units in the pre-treatment step and multi-effect distillation or reverse osmosis plus membrane distillation, coupled with NaCl crystallization, in the concentration step. The relevant techno-economic models have been implemented in Python and integrated in a common simulation platform (*Remote Component Environment, RCE*) to simulate the entire chains.

As regards the step (a) of the methodology, the techno-economic models of MED and NF units are extensively described in previous works (Micari et al. 2019a, Micari et al. 2019b). The main equations describing the RO and the MD technologies are reported in the supplementary materials of a previous work (Micari et al. 2020). For the reactive crystallizers employed to produce $Mg(OH)_2$ and $CaCO_3$, we set up a simplified model based on mass balances under the assumption of a conversion of 100% of the dissolved cations into minerals. Also, we implemented a simplified model for the other two crystallizers, used to produce $CaSO_4$ and NaCl. We employed mass and energy balances to define the amount of crystals produced, the thermal energy required and the outlet flow rates. The fundamental equations used for the four crystallizers are reported in the supplementary materials.

Concerning the step (b) about the definition of the inputs, parameters and outputs of the models, the main inputs about the composition and flow rate of the solution fed to the treatment chains are reported in section 3. Also, the parameters relevant to the different technologies have been taken from the literature or found via sensitivity analyses.

Paragraph 2.2 deals with the step (c) and in particular the development of integrated processes: it extensively describes the five treatment chains analysed in this work. The details about the integration on RCE are given in (Micari et al. 2020).

Finally, the definitions of the global outputs (step (d)) used for the comparison of the chains are reported in paragraph 2.3.

2.2 Description of the treatment chains (step (c))

This paragraph is devoted to describing the five treatment chains analysed in this work. The first chain, represented in Figure 2, is taken as a reference and the others are presented in terms of their differences with respect to the first.

All chains present a pre-treatment and a concentration phase. The pre-treatment part of the first chain includes two nanofiltration units in series: the permeate of the first NF unit is fed to the second NF unit to remove the bivalent ions almost completely. The retentates produced by the two NF units are mixed and sent to a three-step crystallization train. In the first crystallization unit, $Mg(OH)_2$ is produced by adding an alkaline solution; in the second, $CaSO_4$ precipitates from a supersaturated solution; and in the third, limestone ($CaCO_3$) is produced by adding a solution of Na_2CO_3.

The aim of the crystallization train consists in removing the bivalent ions contained in the two retentate solutions and in producing valuable materials. More in detail, the first crystallizer employs a water solution of dolime as alkaline reactant. The dolime is given by the calcination of dolomite that is a mixture of calcium and magnesium carbonates. The calcination process consists in heating the dolomite up to high temperatures, at which the dolomite decomposes into MgO and CaO and CO_2 gas is released (Jakić 2016). Thus, the dolime suspension contains Mg^{2+} and Ca^{2+} ions in equal molar concentration, as in the

dolime, and OH⁻ ions, given by the reaction of the oxides with water. Since the alkaline solution itself contains Mg^{2+} ions, the yield in $Mg(OH)_2$ is doubled and the effluent solution is enriched in Ca^{2+} ions.

The abundance of calcium and sulphate ions makes the effluent supersaturated in $CaSO_4$. The solubility of $CaSO_4$ is quite low and its saturation concentration is equal to 0.0049 mol/l at ambient temperature. The amount of $CaSO_4$ crystals produced in the 2nd crystallizer is calculated by assuming that the outlet solution has to be at the saturation concentration and no heat is supplied to evaporate water. Thus, the global mass balance for this crystallizer presents only the inlet solution, the effluent and the crystals flow rate.

The 2nd crystallizer outlet solution is still rich of Ca^{2+} ions, which are supposed to be completely removed by letting the solution react with a solution of Na_2CO_3 to produce $CaCO_3$ in the last crystallization step. The 3rd crystallizer effluent, rich in NaCl, is mixed with the 2nd NF permeate and the mixture is sent to the concentration phase.

In the first chain, the concentration growth occurs in two combined technologies put in series: RO and MD. The concentrations of the bivalent ions in the concentration stage are much lower than the saturation points of the species which are typically responsible of fouling, such as calcium sulphate or magnesium sulphate. Even in the recovery heat exchangers of the MD unit, the calculated concentration of $CaSO_4$ is lower than the saturation point at the highest temperature (80°C), thus the risk of scaling can be neglected.

The MD retentate is sent to the end crystallizer to produce NaCl crystals. To estimate the maximum amount of NaCl crystals producible in the end crystallizer, we considered two conditions to be fulfilled: (i) the amount of Ca^{2+} and Mg^{2+} should not exceed a certain concentration in order to ensure the effectiveness of the end-crystallizer (Turek et al. 2008) and (ii) the moles of SO_4^{2-} should be limited by the saturation concentration of Na_2SO_4, since Na^+ is so more abundant than Ca^{2+}, that the saturation point might be reached before the gypsum one. In this 1st chain, since the effluent of the 2nd crystallizer is a saturated solution of $CaSO_4$ and the third-crystallizer effluent is mixed with the NF permeate and sent to the RO unit, the second condition on the sulphate concentration is stricter and defines the amount of produced crystals.
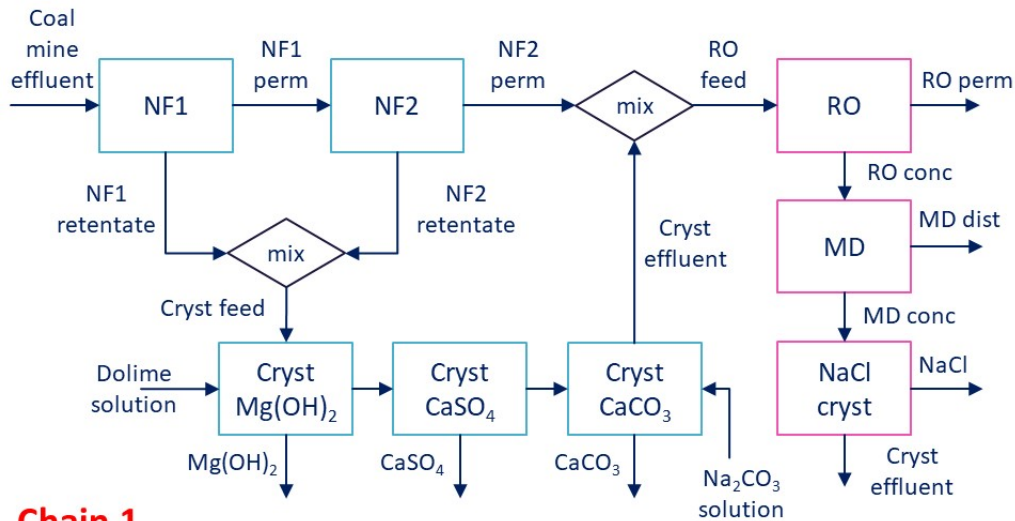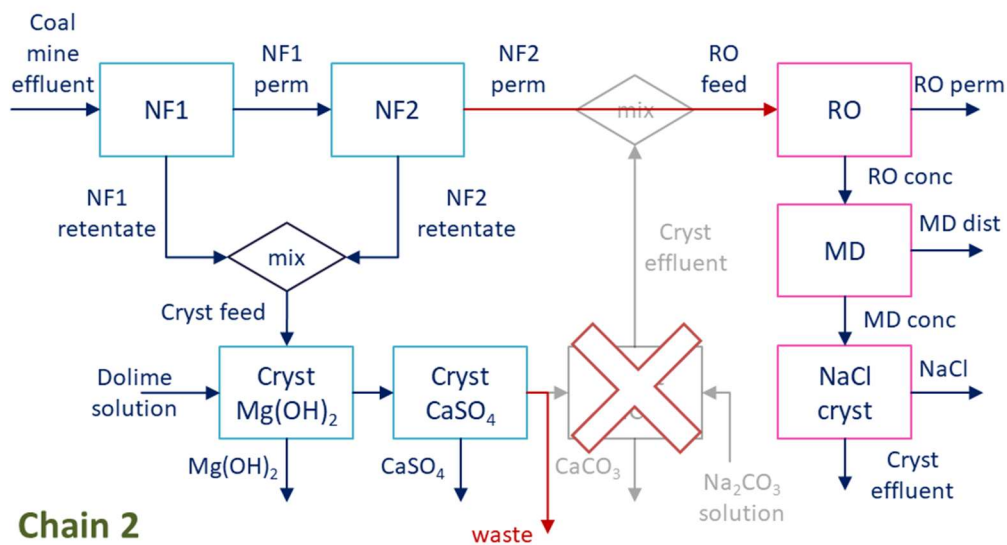
Figure 2. Schematic representation of the first treatment chain (2NF-3cryst-RO-MD-cryst chain). Pre-treatment units are indicated in light blue; concentration units are indicated in purple.

The difference between the first and the second treatment chain stays in the pre-treatment part: the second chain, depicted in Figure 3, presents only two crystallization steps, the first to produce $Mg(OH)_2$ and the second to produce $CaSO_4$. Also, the effluent of the second crystallization step is disposed as a waste (at a certain cost) and not mixed with the NF permeate. Thus, the feed solution sent to the concentration step has lower flow rate and lower concentration of NaCl and bivalent ions. Thus, also in this case, the risk of scaling in the concentration units can be neglected.

Concerning the conditions to define the amount of NaCl crystals produced in the end crystallizer, the first condition on the maximum amount of bivalent cations is stricter since the SO_4^{2-} ions are more rejected than Ca^{2+} and Mg^{2+} in the two NF units.

Figure 3. Schematic representation of the second treatment chain (2NF-2cryst-RO-MD-cryst chain). Pre-treatment units are indicated in light blue; concentration units are indicated in purple.

The other three chains present a concentration step based only on MED.

The difference between the first and the third system is in the concentration step: while the concentration step in the first chain is performed via RO-MD combination, in the third chain (in Figure 4) a MED plant is responsible for the whole concentration rise. In this chain, even if the concentration of components possibly responsible of scaling is always lower than their saturation point, the problem of scaling is more likely to occur and it may be more damaging since the feed evaporation takes place on the external surface of the tube bundle (Al-Rawajfeh et al. 2005). Therefore, suitable Top Brine Temperatures (TBT) and number of effects of the MED plant have been defined to minimize the risk for scaling. These are reported in section 3. Concerning the end-crystallizer, as in the 1st chain, the condition on the maximum sulphate concentration in the crystallizer effluent is stricter.
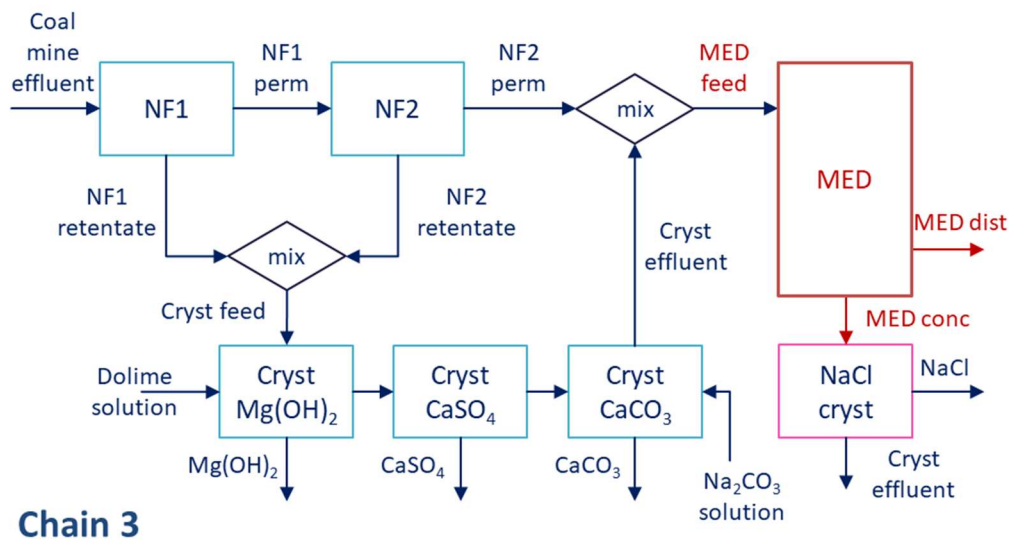

Figure 4. Schematic representation of the third treatment chain (2NF-3cryst-MED-cryst chain). Pre-treatment units are indicated in light blue; concentration units are indicated in purple.

In the 4th chain (Figure 5), both pre-treatment and concentration steps are different than those of the 1st chain. The pre-treatment is composed of two NF units and two crystallizers to produce $Mg(OH)_2$ and $CaSO_4$ and the 2nd crystallizer effluent is disposed as a waste, analogously to the 2nd chain. The concentration step presents the MED plant, coupled with an end-crystallizer to produce NaCl crystals. In this case, the amount of bivalent ions present in the NF permeate fed to the MED can be neglected and a higher TBT is allowed. In the calculation of the produced NaCl crystals, the maximum amount is limited by the concentration of bivalent cations.
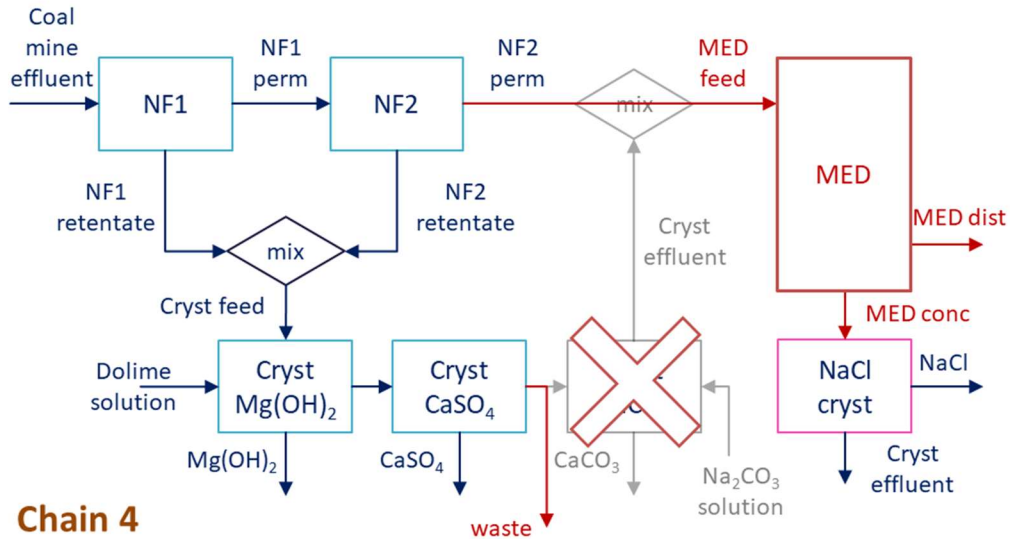
Figure 5. Schematic representation of the fourth treatment chain (2NF-2cryst-MED-cryst chain). Pre-treatment units are indicated in light blue; concentration units are indicated in purple.

Finally, the 5th chain, sketched in Figure 6, presents a third NF stage in the pre-treatment step. This is included to further treat the mixture of the NF permeate and the crystallizer effluent, before being fed to the concentration step. The third NF unit is supposed to behave similarly to the second one, thus, equal NF membrane rejections, feed pressure and recovery are considered. The 3rd NF retentate constitutes a waste to be disposed with a certain cost. Analogously to the 4th chain, the content of bivalent ions in the MED feed is negligible since it is abated in the NF. Therefore, higher Top Brine Temperatures can be used also in this case. Moreover, analogously to the 3rd chain, the condition on the sulphate concentration is the strictest condition to estimate the maximum amount of producible NaCl crystals.
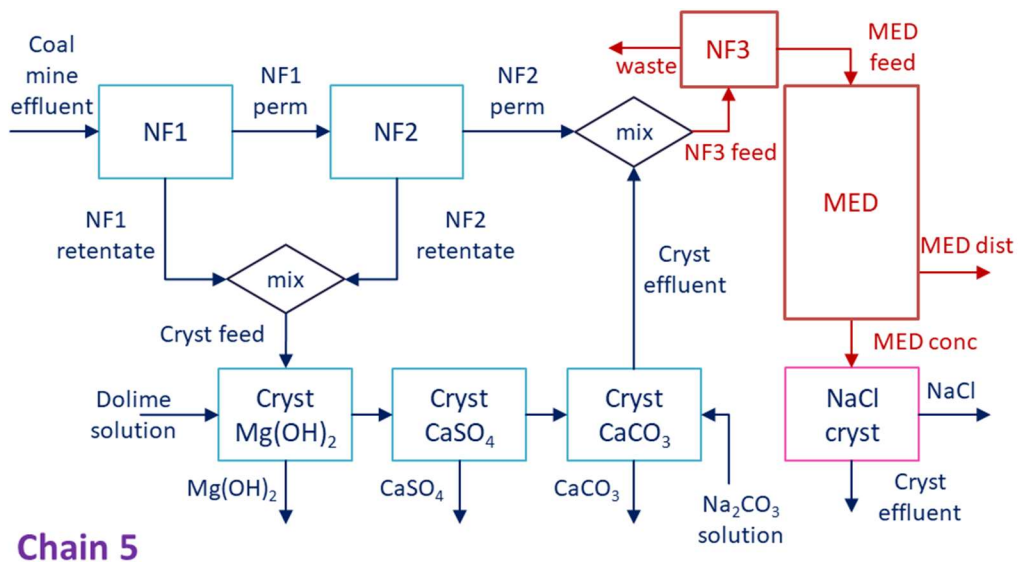

Figure 6. Schematic representation of the fifth treatment chain (3NF-3cryst-MED-cryst chain). Pre-treatment units are indicated in light blue; concentration units are indicated in purple.

The main features of the five proposed treatment chains are summarized in Table 1.

Table 1. Main components of the five treatment chains.

Chain	Pre-treatment: nanofiltration	Pre-treatment: crystallization	Concentration step
1	2 units, permeate staging	3 units: $Mg(OH)_2$, $CaSO_4$ and $CaCO_3$	RO-MD + end-crystallizer
2	2 units, permeate staging	2 units: $Mg(OH)_2$, $CaSO_4$	RO-MD+ end-crystallizer
3	2 units, permeate staging	3 units: $Mg(OH)_2$, $CaSO_4$ and $CaCO_3$	MED+ end-crystallizer
4	2 units, permeate staging	2 units: $Mg(OH)_2$, $CaSO_4$	MED+ end-crystallizer
5	2 units, permeate staging + 1 unit before concentration step	3 units: $Mg(OH)_2$, $CaSO_4$ and $CaCO_3$	MED+ end-crystallizer

2.3 Main economic parameters and global output values

The proposed chains are analysed from the economic point of view via the calculation of the capital and operating expenditures (CAPEX and OPEX) of every unit. The annualized capital costs are calculated by assuming different depreciation periods, depending on the technology, and a common discount rate of 6% (Kesieme et al. 2013, Papapetrou et al. 2017). The economic models employed for the NF and the MED processes have been described elsewhere (Micari et al. 2019a, Micari et al. 2019b). Concerning the RO unit, the capital costs include the cost for the membrane elements and the pressure vessels, the high-pressure pump, piping and intake. These were annualized by assuming a depreciation period of 25 years (Vince et al. 2008). The operating costs take into account electricity, labor, maintenance (estimated at the 3%/y of the investment plus 20% of the labor cost), chemicals and membrane replacement cost (with a replacement rate of 15% per year) (Wilf 2007, Vince et al. 2008).

Regarding the MD unit, the investment costs of the modules, the pumps and the heat exchangers are calculated, together with the costs for intake and pretreatment (Al-Obaidani et al. 2008). The total investment cost is annualized assuming a depreciation period of 10 years (Hitsov et al. 2018). Conversely, the operating costs take into account the electric and thermal energy costs, the maintenance cost (calculated as the 2.5%/y of the investment cost minus the cost of membranes and modules), the labor cost, the chemicals and the membrane replacement cost (with a replacement rate of 15% per year) (Al-Obaidani et al. 2008, Hitsov et al. 2017).

The capital cost of each crystallization stage includes the cost of the crystallizer and of a disc and drum filter, calculated via the Module Costing Technique as function of their volume and area, respectively (Turton et al. 2012). The capital costs are annualized assuming a depreciation period of 20 years. The operating costs account for the pumping costs and the cost of the reactant, in the case of the crystallization of $Mg(OH)_2$ and $CaCO_3$, or of the thermal energy, in the case of the NaCl crystallizer.

Conservatively, we assumed that the salvage value of the technologies at the end of the project lifetime was equal to zero.

The most relevant terms of cost used in the economic analysis are reported in Table 2. The electricity cost is the cost for non-household consumers in Poland (Eurostat 2019), while the thermal energy cost is estimated for the case of low-temperature waste heat available in the industrial site (Micari et al. 2019b).

Table 2. Main specific terms of cost and revenues used for the economic analysis of the treatment chains. The costs of the chemicals used as reactant or produced as by-products are taken from (U.S. Department of the Interior 2017).

Main specific terms of cost and revenues			
Terms of cost	NF membrane (Drioli et al. 2006)	30	$/m^3
	Dolime (Humphries et al. 2019)	60	$/ton
	Na_2CO_3	275	$/ton
	Brine disposal (Kesieme et al. 2013)	0.04	$/m^3
	RO element (Wilf 2007)	450	$/element
	MD module (Hitsov et al. 2018)	1000	$/module
	MD membrane (Hitsov et al. 2018)	60	$/m^2
	Thermal energy cost	0.01	$/kWh$_{th}$
	Electricity cost	0.103	$/kWh$_{el}$
Terms of revenue	$Mg(OH)_2$	1200	$/ton
	$CaSO_4$	40	$/ton
	$CaCO_3$	300	$/ton
	Pure water (Mezher et al. 2011)	1	$/m^3

Finally, in order to compare the systems, a global output value is introduced under the name of Levelized Cost of Salt (LSC) in [$/ton$_{NaCl}$]. The LSC is the cost that the produced NaCl crystals would have to allow the project to break-even at the end of its lifetime. This is defined in analogy with the Levelized Water Cost (LWC) used as a reference parameter for the desalination plants (Papapetrou et al. 2017). In this work, the LSC is defined as follows:

$$LSC \left[\frac{\$}{ton}\right] = \frac{CAPEX_{chain} + OPEX_{chain} - Revenue_{water} - Revenue_{minerals} \left[\frac{\$}{y}\right]}{NaCl \; crystals \; produced \left[\frac{ton}{y}\right]}$$

3. DESCRIPTION OF THE CASE STUDY

All the analyses presented in this work have been performed considering a fixed flow rate and composition of the coal mine effluent to be treated. In particular, the inlet feed flow rate is always equal to 100 m^3/h, that is in line with the produced volumes of highly concentrated coal mine effluents mentioned in the literature (Turek et al. 2005b). The inlet composition is reported in Table 3.

Table 3. Composition of the coal mine effluent of the present case study.

Ion	C [mol/m^3]	C [g/l]
Na$^+$	358	8.25
Cl$^-$	383	13.4
Mg^{2+}	11.7	0.28
Ca^{2+}	8.51	0.34
SO$_4^{2-}$	7.71	0.77

The operating conditions of the units in the treatment chains have been given through suitable sets of parameters. These are taken from literature (e.g. the rejection of NF membranes) or from novel sensitivity analyses carried out with the single models (e.g. the number of effects of the MED plant).

Regarding nanofiltration, all chains include at least two NF units to reduce as much as possible the content of bivalent ions in the permeate. Typical NF membrane rejections taken from literature are employed (Turek et al. 2018), as reported in Table 4. The values of feed pressure and recovery are fixed for all simulations and equal to 30 bar and 80% in the first stage and 50 bar and 80% in the second stage. In the 5th chain, the third NF unit is supposed to have the same operating conditions as the second NF unit (feed pressure of 50 bar and recovery of 80%).

Table 4. Rejection values of NF membranes used in the 1st and in the 2nd stage in all simulation. The rejection values of NF membranes in the 3rd stage (in the 5th chain only) are equal to those of the 2nd stage.

Ion	Rejection 1st stage [-]	Rejection 2nd stage [-]
Na$^+$	0.06	0.3
Cl$^-$	0.2	0.45
Mg^{2+}	0.8	0.98
Ca^{2+}	0.7	0.97
SO$_4^{2-}$	0.98	0.98

Concerning the concentration steps, the outlet concentrations of the desalination units (i.e. either RO+MD or MED) are constant, since the concentration of the feed of the end-crystallizer has to be 250,000 ppm in all cases. This concentration value was obtained on the basis of preliminary techno-economic analyses aimed at minimizing the sum of capital and operating costs of the chain. In the first two chains, the RO unit is responsible for the concentration growth up to the maximum achievable concentration, i.e. 70,000 ppm. The limit on the concentration achievable in the RO depends on the limits on the maximum applicable pressure (Kesieme et al. 2013). Thus, the RO retentate is sent to the MD unit that has to concentrate it up to 250,000 ppm. Conversely, in the other three chains, MED is responsible for the whole concentration increase, up to 250,000 ppm.

The RO plant is composed by two stages: in the first, the vessels in parallel contain 8 modules in series and in the second, they contain 6 modules. The MD plant is composed by modules arranged in parallel and in series. Each module presents six MD membranes wounded together in a parallel configuration. The inlet temperatures of the feed and the permeate solutions in the direct contact MD are fixed at 80°C and 20°C, respectively (Hitsov et al. 2018).

Concerning the temperature of the inlet steam in the MED plant, this depends on the composition of the feed solution and the risk of scaling due to the presence of bivalent ions. Since the MED feed of the 3rd chain presents a higher amount of bivalent ions, the temperature of the steam is fixed at 70°C, in order to have a Top Brine Temperature (TBT) lower than 70°C. Conversely, in the other two chains, the risk of scaling is negligible and the temperature of the steam is fixed at 100°C. The TBT determines the number of effects that minimizes the total MED costs. The techno-economic model of the MED plant was run to find the number of effects corresponding to the minimum total cost (i.e. the sum of CAPEX and OPEX) (Micari et al. 2019b). In particular, the optimum number of effects resulted to be 7 for the 3rd and the 4th chains and 9 for the 5th chain.

4. RESULTS AND DISCUSSION

In this section, firstly, the results of the energetic and economic analysis of the single units included in the chains are reported. Secondly, the chains are compared in terms of total electric and thermal energy demand, LSC and NaCl salt recovery. Finally, the results of sensitivity analyses are shown to investigate how much the LSC values of the five systems are affected by the market value of the by-products and by the specific costs of energy.

4.1 Energetic and economic analysis of each chain

The energy requirements of the five presented chains are reported in Figure 7. In all cases, the thermal energy required by the main concentration stage (i.e. the MD unit in the first two chains and the MED unit in the other three) is prominent. As a matter of fact, MD and MED are responsible for a very significant concentration change and the distillate that has to be produced is more than 70% of the inlet feed.

The thermal energy requirement of the main concentration stage depends on its feed flow rate and concentration. Concerning the chains with MD (pie chart on the left in Figure 7), the MD feed concentration is always the same and the feed flow rate is lower in the 2nd chain. Thus, the fraction of the MD thermal energy is lower in the 2nd than in the 1st chain. Conversely, in the chains with MED and two NF units (pie chart on the right in Figure 7), two effects have to be accounted: on the one hand, the MED feed flow rate in the 4th chain is lower, but on the other hand, the inlet concentration of MED feed is lower and the total concentration factor is higher. Therefore, the fraction of MED thermal energy is slightly lower in the 3rd than in the 4th chain. Also, in the chains where the effluent of the crystallizer is sent to the concentration stage (1st and 3rd), the second term per relevance is the thermal energy required by the end-crystallizer to produce NaCl crystals. Conversely, in the chains with only two crystallization steps (2nd and 4th), the second term per relevance is the total electric demand of the NF units. In these cases, the thermal demand of the NaCl crystallizer is lower, because of its lower feed flow rate.

Concerning the 5ᵗʰ chain, although MED thermal energy again represents the main term, the fraction covered by the other units, in particular by the three NF units and the NaCl crystallizer, is much higher than in the other chains. In this regard, the third NF unit plays a key role, because it operates at higher pressure with a higher flow rate in comparison with the other two NF units.
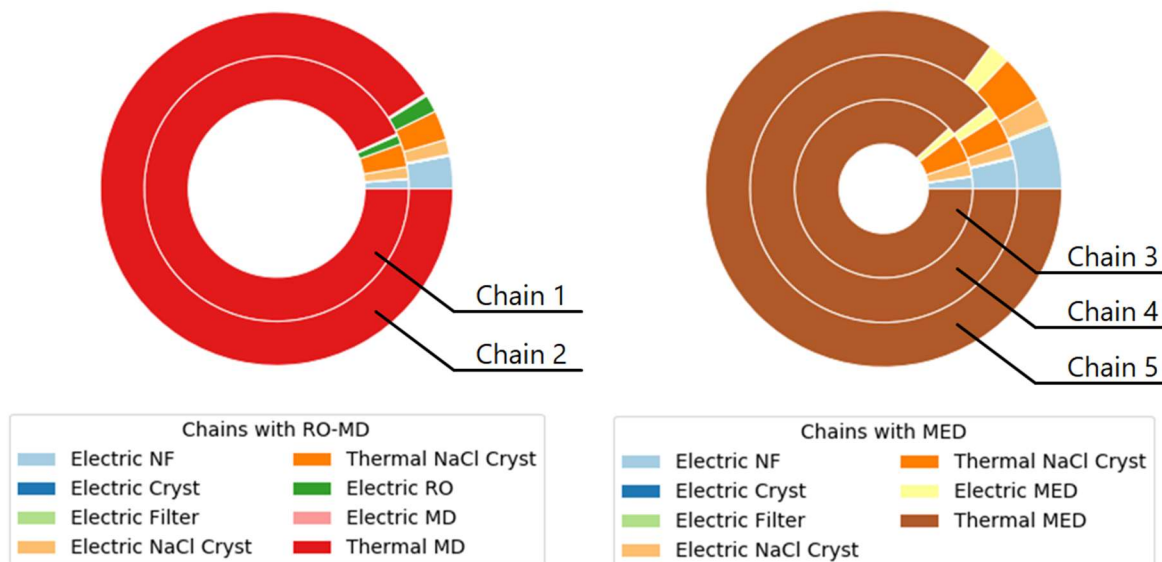

Figure 7. Nested pie charts representing the energy requirements of the five treatment chains.

Furthermore, we carried out a detailed economic analysis of the five treatment chains. The bar charts in Figure 8 show the capital and operating costs and the revenue given by the by-products for the five chains.

The OPEX of the main concentration stage is always the most significant term, except for the 5ᵗʰ chain where the total OPEX of the NF units turns out to be higher than the OPEX of MED. In the first two chains, the MD operating costs are the most significant expenditures, especially in the 1ˢᵗ chain, where the MD feed flow rate is higher. In the 3ʳᵈ and the 4ᵗʰ chain, the OPEX of MED is the highest term, even if in the 4ᵗʰ chain it is comparable with the costs of NF. Moreover, the chains without recycle of the crystallizer effluent (2ⁿᵈ and 4ᵗʰ) present lower capital and operating expenses of the concentration stage, including the NaCl crystallizer, because of the lower feed flow rate. These chains have also reduced crystallization costs, since they present only two crystallization steps. Concerning the 5ᵗʰ chain, the presence of an additional NF unit operating at a higher pressure and flow rate makes the total capital and operating costs of the NF units the highest expenditures. Also, it is worth noting that the costs of the MED unit and of the NaCl crystallizer are intermediate between those of the 3ʳᵈ and the 4ᵗʰ chain. This is because the flow rate fed to the MED is given by the permeate of NF3, which is higher than the feed flow rate of the 4ᵗʰ chain but lower than the total flow rate fed to the MED in the 3ʳᵈ chain (since the recovery of NF3 is 80%, the MED feed flow rate is 80% of the MED feed flow rate of the 3ʳᵈ chain).

Concerning the revenues, the main term is always the one due to the production of $Mg(OH)_2$ in the crystallizer and it is followed by the revenue due to the water production. With this regard, a significant amount of water is produced to concentrate the solution up to the saturation point and the relevant revenues have an important role. In the chains with two NF

units and three crystallization steps with RO-MD (1st chain) and with MED (3rd chain), the OPEX of the concentration stage is higher than the revenues given by $Mg(OH)_2$ production. Conversely, in the others, the $Mg(OH)_2$ revenues offset the operating costs due to the thermal requirement of the concentration step. However, it has to be said that the global revenues of the chains with two crystallization steps are lower, because $CaCO_3$ production is missing and less water is produced in the concentration step.

Overall, for all chains, the operating costs are mostly given by the energy costs. However, MED has always lower thermal consumptions than MD and consequently lower costs, although it is responsible for a larger concentration rise.
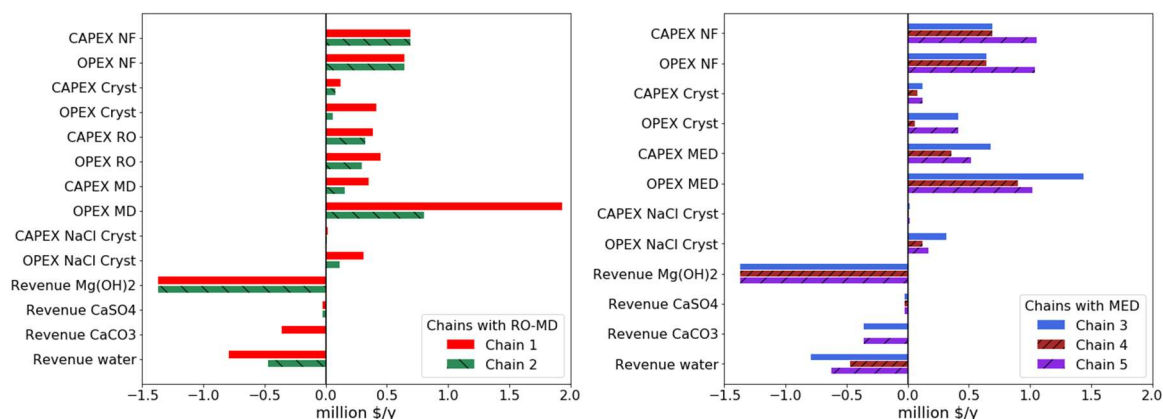

Figure 8. Bar charts with the CAPEX, OPEX and revenues (negative) of the five treatment chains.

4.2 Comparison of the representative output values of the five systems

The aim of this paragraph is to compare the chains via global outputs, used to represent their technical and economic performances. Firstly, the chains are compared in terms of their outlet flow rates of minerals and water, depicted in Figure 9. The chart shows that the water production varies from one chain to the other and the highest production of water occurs in the chains with two NF units and three crystallization steps (1st and 3rd chains), because a higher flow rate is sent to the concentration step. Conversely, the chains with two NF units and two crystallization steps (2nd and 4th chains) show the lowest water production, because part of the water is lost with the effluent of the second crystallizer, which is disposed as a waste. The 5th chain, with three NF units and three crystallization steps, presents an intermediate water production, because the 3rd NF unit leads to an intermediate MED feed flow rate between those of the 3rd and the 4th chain. Remarkably, the production of $Mg(OH)_2$ and $CaSO_4$ is the same in all systems, since the composition of the feed is constant and the relevant crystallization steps are present in every system and behave in the same way. On the contrary, crystals of $CaCO_3$ are produced only in the 1st, the 3rd and the 5th chain because in the other two the corresponding crystallizer is not included.
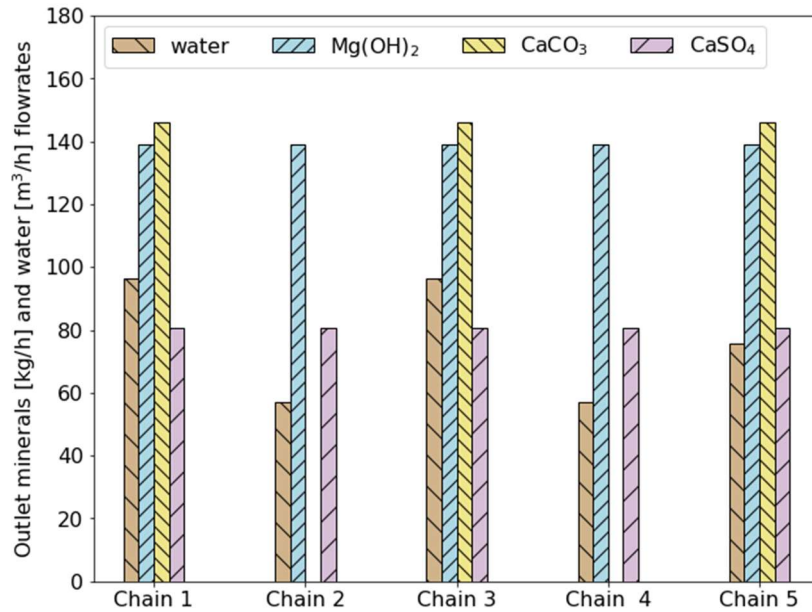
Figure 9. Outlet flow rates of the minerals (Mg(OH)$_2$, CaCO$_3$ and CaSO$_4$) [kg/h] and of water [m^3/h] for the five chains.

Secondly, we compared the amount of NaCl crystals produced in the chains by defining the NaCl recovery, which represents the percentage of the inlet NaCl that is converted into crystals in the end-crystallizer. The values of NaCl recovery for the 5 chains are reported in Figure 10. The 1st and the 3rd chains ensure an almost total recovery of NaCl, since these are devised with the aim to minimize the losses of NaCl. In both cases, the limit on the maximum amount of NaCl crystals, which corresponds to the minimum effluent flow rate in the end crystallizer, is defined on the basis of the maximum concentration of SO$_4^{2-}$ to avoid the precipitation of Na$_2$SO$_4$. Chains 2 and 4 have a lower NaCl recovery, around 37%, since most of the salt is lost with the crystallizer effluent that is not sent to the concentration step. In the 5th chain, the NaCl recovery is around 50%, because a certain amount of Na$^+$ and Cl$^-$ ions is lost with the retentate of the third NF step, whose membranes have a rejection toward Na$^+$ and Cl$^-$ of around 30%. Thus, the 3rd NF allows for operating the MED at the highest top brine temperature without risks of scaling but the disposal of its retentate leads to a certain loss of NaCl.
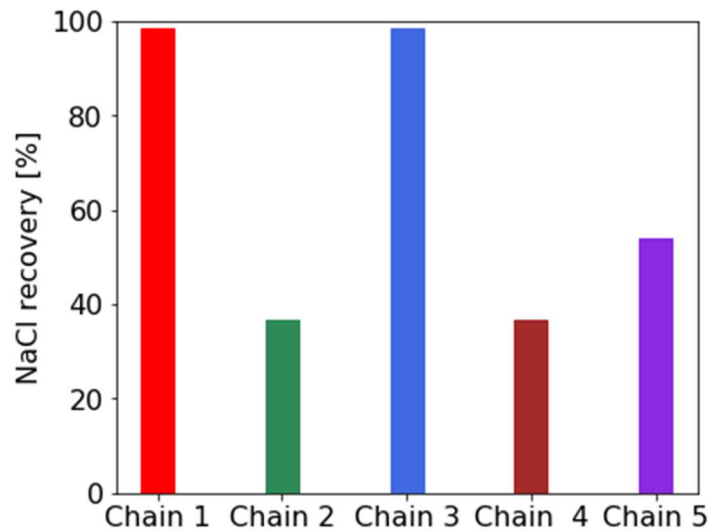
Figure 10. Values of NaCl recovery [%] for the five chains.

Furthermore, the total electric and thermal energy demand of the five systems are assessed and compared in Figure 11.

The electricity demands of the chains with two NF units and two crystallizers (chains 2 and 4) are significantly lower than those with two NF units and three crystallizers (chains 1 and 3). This is due to the lower feed flow rate in the concentration step, which is the most energy-intensive phase. Moreover, it is not surprising that the chains with the RO-MD coupling (1st and 2nd) have higher electricity consumption than the chains with MED (3rd and 4th), because RO is the most electricity-intensive unit with a specific demand between 3 and 4 kWh_{el}/m^3_{dist}. In addition, MD has a specific electric demand of around 1.8 kWh_{el}/m^3_{dist}. Conversely, MED has a specific electricity demand of 1.5 kWh_{el}/m^3_{dist}. The 5th system presents a total electricity demand comparable with the one of the 3rd chain and this is mostly due to the additional electric energy requirement of the third NF step.

Concerning the thermal demand, the 1st chain has the highest demand, because of the high thermal consumption of the MD unit. Notably, the difference between the chains with RO-MD is much more enhanced than that between the chains with MED. In the first two chains, the MD feed has the same inlet concentration (i.e. 70,000 ppm) and different flow rate: since the flow rate is almost three times higher in the 1st chain, the corresponding total thermal demand increases proportionally. Conversely, the MED feed in the 3rd chain has higher flow rate, but also higher concentration with respect to the MED feed in the 4th chain. The smaller concentration growth to be performed in the MED in the 3rd chain partially counterbalances the higher flow rate and this leads to a slighter difference between the two MED chains.

Concerning the 5th chain, the heat demand is found to be similar to that of chain 4. In this case, the MED feed concentration and flow rate are intermediate between those of the 3rd and the 4th chains. However, the employed number of effects is higher (equal to 9) than the one used for the other two chains (equal to 7), so the specific heat demand as well as the total thermal energy demand turns out to be lower. As already mentioned, the choice of the number of effects is performed in order to minimize the total costs (e.g. the sum of CAPEX and OPEX of MED): in the last chain, the optimum number of effects is higher because, at the

same steam temperature, the concentration factor is lower, so the capital costs are significantly lower.
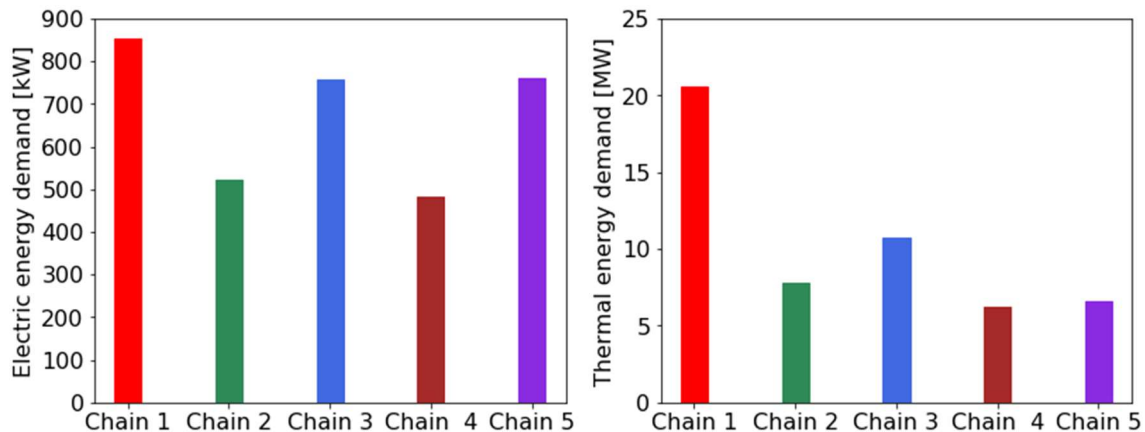

Figure 11. Total electric (left) and thermal (right) energy demand values of the five chains. All have a total capacity in terms of feed flow rate to be treated equal to 100 m³/h.

From the economic point of view, the systems are compared through the estimation of the levelized cost of the main product of the chain, the NaCl salt. The values of LSC for the five chains are reported in Figure 12. Firstly, it is evident that the chains where the crystallizer effluent is sent to the concentration step (Chains 1 and 3) are more economically feasible than those presenting only two crystallizers, in which the effluent of the second is disposed (Chains 2 and 4). Secondly, the RO-MD chains (1st and 2nd) result to have a higher LSC with respect to the corresponding MED ones (3rd and 4th). Therefore, it is possible to conclude that the MED technology, less heat-intensive than the MD, allows for devising cheaper solutions.

Finally, in the 5th chain, the inclusion of an energy-intensive third NF step and a significant loss of NaCl in the disposed NF retentate make the chain the least economically feasible.

The obtained values of LSC are compared with the typical market values of high purity (99.5%) NaCl salt, which can vary between 80 and 150 $/ton$_{NaCl}$ (U.S. Department of the Interior 2017). This area is highlighted in grey in Figure 12.

The LSC found for the chains with MED and two NF units (Chain 3 and 4) result to fall within this area and this finding can be used to confirm the feasibility of these treatment processes. In particular, the 3rd chain is the most economically feasible with a LSC value of around 90 $/ton$_{NaCl}$. Notably, the LSC of the 1st chain is slightly higher than 150 $/ton$_{NaCl}$, thus further technological improvements can easily make this chain competitive with the market value of NaCl crystals.
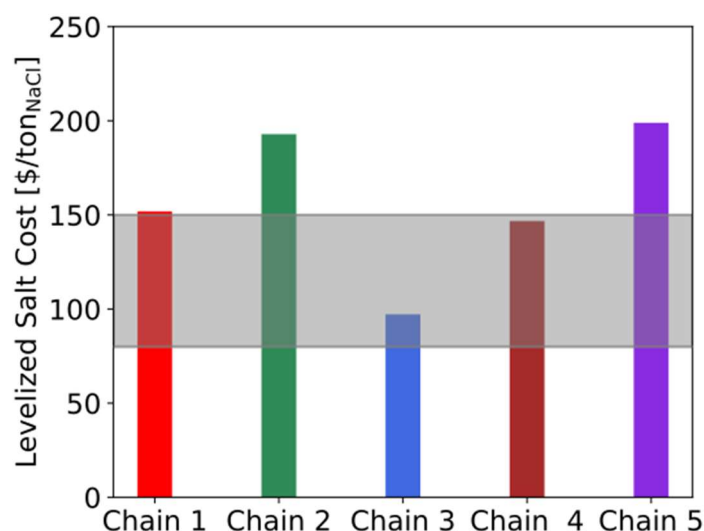
Figure 12. Levelized Salt Cost (LSC) calculated for the five chains. The grey area corresponds to the range of market values of NaCl crystals with high purity (99.5%).

4.3 Sensitivity analyses

A sensitivity analysis is performed by varying the selling prices of the by-products and the cost of electricity and thermal energy. The variation range goes from -50% to +50% of the reference prices and costs reported in Table 2. Simulations are performed for every chain by varying one economic parameter per time, while the others are kept equal to the reference ones (Table 2). Figure 13 (left) shows the LSC variation for the five investigated chains when the price of $Mg(OH)_2$ is varied between 600 and 1800 \$/ton, the price of $CaCO_3$ is varied between 150 and 450 \$/ton (only for the chains with three steps of crystallization, i.e. the 1st, 3rd and 5th) and the price of water is varied between 0.5 and 1.5 \$/m^3. The results are depicted in bar plots, showing the range of variation of the LSC with respect to the reference (value highlighted in the middle).

In all cases, the most significant LSC variation occurs when the price of $Mg(OH)_2$ is varied. This is due to the fact that, as a rule, the revenues due to the magnesium hydroxide production constitute one of the most significant term in the costs breakdown of each chain.

With this regard, the range of variation of the LSC in the 2nd and 4th chain is much wider than one found for the 1st and the 3rd chain. As a matter of fact, the lowest LSC values obtained at the highest $Mg(OH)_2$ price in chains 2 and 4 are even lower than the corresponding ones of chains 1 and 3, respectively. As shown in the costs breakdown of the chains in which the effluent of the second crystallizer is disposed (2nd and 4th chains in Figure 8), $Mg(OH)_2$ revenues have an absolute value significantly higher than all the other terms, also because the concentration processes are fed by a lower flow rate. Thus, the variation of $Mg(OH)_2$ price has a major impact on the total costs in these cases. However, it has to be said that the amount of $Mg(OH)_2$ produced is the same in all chains, thus it has to be expected that the systems with a higher production of NaCl salt (chains 1 and 3) show a slighter variation of the levelized salt cost with respect to the chains with a lower NaCl production, when a certain annual term of cost or revenue is changed of the same amount.

On the contrary, the amount of water produced by the chains is different, thus these variously respond to water price variations. In particular, the water production is higher in the chains with three crystallization steps (chain 1 and 3). At the same time, the global expenses of these chains are higher and the relative weight of the water revenue in the general cost breakdown is smaller than in the 2nd and the 4th chain. Overall, the LSC variation due to the water cost change is still bigger in the chains where the crystallizer effluent is disposed (2nd and 4th) but comparable with the one found for the other chains (1st and 3rd).

Concerning the impact of $CaCO_3$ price variation, this is bigger in the 5th chain than in the 1st and the 3rd. As mentioned for the $Mg(OH)_2$ price variation, the $CaCO_3$ productivity is the same in the three chains but the variation of LSC is bigger when the NaCl productivity is lower.

Figure 13 (right) reports the LSC values obtained for each chain by varying the cost of the thermal and electric energy. The higher thermal consumption of MD leads to a stronger impact of the thermal energy cost on the RO-MD chains (1st and 2nd). Also, the variation range is larger in the 1st chain than in the 2nd, because of the higher total thermal demand. Conversely, the variation range of the 3rd chain is smaller than that of the 4th chain, because the higher salt production makes the levelized cost more stable. Finally, it was found that the range of LSC variation with the cost of electricity is always slightly smaller than that with the heat cost, except for the 5th chain. As a matter of fact, thermal energy covers the highest share of the energy demand in all chains. Nevertheless, in the last chain, the additional energy requirement of the third NF unit makes the chain slightly more sensitive to electricity cost variations.
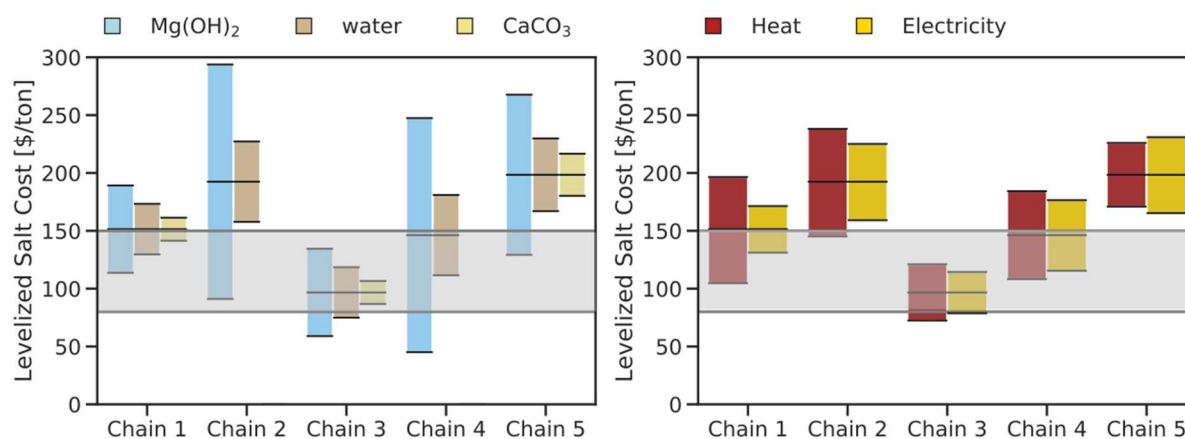

Figure 13. Bar plots representing the sensitivity of the Levelized Salt Cost to the price of $Mg(OH)_2$, $CaCO_3$ and water (left) and to the costs of electricity and heat (right). The upper and lower values of each bar correspond to the LSC found for a variation of the price/cost of +/-50%. The value in the middle is the LSC found in the reference case.

5. CONCLUSIONS

The effluent produced by coal mines is a severe threat to the environment if directly disposed into the rivers. In this work, we devised and analysed five treatment chains to purify the effluent and to recover valuable materials. The chains are composed by a pre-treatment step, given by different combinations of nanofiltration and crystallization units, and a concentration

step, including multi-effect distillation and NaCl crystallizer or reverse osmosis, membrane distillation and NaCl crystallizer.

The analysis of the energy demands and the costs of the chains showed that the thermal energy demand constitutes in all cases the highest fraction of the total demand, especially in the chains with MD. Consequently, the operating costs of the concentration technologies were always among the most crucial expenses. However, in most cases, it was found that the revenues due to $Mg(OH)_2$ production are able to offset the highest expenditures.

The global comparison of the chains was focused on the total energy demands, the NaCl recovery and the levelized cost of the produced salt (LSC). This last parameter allowed for assessing the feasibility of the chain, by comparing it with the current market values of high-purity NaCl crystals. The results showed that the chains devised to maximize the NaCl recovery have higher thermal and electrical energy demand but also lower LSC, thus being more economically feasible. Moreover, the MED technology allowed for strongly reducing the global LSC, because of its lower thermal demand: the lowest LSC was found for the treatment chain with two NF units and three crystallizers in the pre-treatment step and with MED and NaCl crystallizer in the concentration step. For this chain, we found a LSC value of 90 $/ton$_{NaCl}$ that falls within the range of typical high-purity NaCl price (from 80 to 150 $/ton). Therefore, this chain was found to be economically competitive with the market value. Overall, different solutions have been proposed to treat a coal mine effluent and to recover valuable products: water, minerals and NaCl crystals. The findings of this study can have important consequences on the industrial sector of the coal mines, since they can heavily contribute to improve the sustainability of the process, while proposing economically feasible treatment configurations. The proposed chains allow for a strong reduction of the environmental impact of the industrial process by avoiding the disposal of a heavily polluted solution into the environment. Future studies will focus on a detailed assessment of the environmental impact of the proposed configurations, in terms of CO_2 emissions due to construction and operation of the treatment processes.

ACKNOWLEDGEMENTS

NOMENCLATURE

AMD	Acid mine drainage
C	Concentration [mol/m^3 or g/l]
CAPEX	Capital Expenditures [$/y]
Cryst	Crystallizer
LSC	Levelized Salt Cost [$/ton$_{NaCl}$]
LWC	Levelized Water Cost [$/m^3]
MD	Membrane distillation
MED	Multi-effect Distillation

NF   Nanofiltration
OPEX   Operating Expenditures [$/y]
RCE   Remote Component Environment
RO   Reverse Osmosis
TBT   Top Brine Temperature [°C]
TDS   Total dissolved solids

BIBLIOGRAPHY

Akcil, A., and S. Koldas. 2006. Acid Mine Drainage (AMD): causes, treatment and case studies. Journal of Cleaner Production **14**:1139-1145.

Al-Obaidani, S., E. Curcio, F. Macedonio, G. Diprofio, H. Alhinai, and E. Drioli. 2008. Potential of membrane distillation in seawater desalination: Thermal efficiency, sensitivity study and cost estimation. Journal of Membrane Science **323**:85-98.

Al-Rawajfeh, A. E., H. Glade, and J. Ulrich. 2005. Scaling in multiple-effect distillers: the role of CO_2 release. Desalination **182**:209-219.

Baruah, B. P., and P. Khare. 2010. Mobility of trace and potentially harmful elements in the environment from high sulfur Indian coal mines. Applied Geochemistry **25**:1621-1631.

Christensen, B., M. Laake, and T. Lien. 1996. Treatment of acid mine water by sulphate reducing bacteria; results from a bench scale experiment. Water Research **30**:1617-1624.

Dharmappa, H. B., K. Wingrove, M. Sivakumar, and R. Singh. 2000. Wastewater and stormwater minimisation in a coal mine. Journal of Cleaner Production **8**:23-34.

Drioli, E., E. Curcio, G. Di Profio, F. Macedonio, and A. Criscuoli. 2006. Integrating Membrane Contactors Technology and Pressure-Driven Membrane Operations for Seawater Desalination. Chemical Engineering Research and Design **84**:209-220.

Ericsson, B., and B. Hallmans. 1996. Treatment of saline wastewater for zero discharge at the Debiensko coal mines in Poland. Desalination **105**:115-123.

Eurostat. 2019. Electricity prices for non-household consumers - bi-annual data (from 2007 onwards).

Feng, D., C. Aldrich, and H. Tan. 2000. Treatment of acid mine water by use of heavy metal precipitation and ion exchange. Minerals Engineering **13**:623-642.

Gibert, O., J. de Pablo, J. L. Cortina, and C. Ayora. 2002. Treatment of acid mine drainage by sulphate-reducing bacteria using permeable reactive barriers: A review from laboratory to full-scale experiments. Re/Views in Environmental Science & Bio/Technology **1**:327–333.

Hitsov, I., L. Eykens, W. D. Schepper, K. D. Sitter, C. Dotremont, and I. Nopens. 2017. Full-scale direct contact membrane distillation (DCMD) model including membrane compaction effects. Journal of Membrane Science **524**:245-256.

Hitsov, I., K. D. Sitter, C. Dotremont, and I. Nopens. 2018. Economic modelling and model-based process optimization of membrane distillation. Desalination **436**:125-143.

Humphries, T. D., K. T. Møller, W. D. A. Rickard, M. V. Sofianos, S. Liu, C. E. Buckley, and M. Paskevicius. 2019. Dolomite: a low cost thermochemical energy storage material. Journal of Materials Chemistry A **7**:1206-1215.

Jakić, J. 2016. Characterization of Dolomitic Lime as the Base Reagent for Precipitation of $Mg(OH)_2$ from Seawater. Chemical and Biochemical Engineering Quarterly Journal **30**:373-379.

Kalin, M., A. Fyson, and W. N. Wheeler. 2006. The chemistry of conventional and alternative treatment systems for the neutralization of acid mine drainage. Sci Total Environ **366**:395-408.

Kefeni, K. K., B. B. Mamba, and T. A. M. Msagati. 2017a. Magnetite and cobalt ferrite nanoparticles used as seeds for acid mine drainage treatment. J Hazard Mater **333**:308-318.

Kefeni, K. K., T. A. M. Msagati, and B. B. Mamba. 2017b. Acid mine drainage: Prevention, treatment options, and resource recovery: A review. Journal of Cleaner Production **151**:475-493.

Kesieme, U. K., N. Milne, H. Aral, C. Y. Cheng, and M. Duke. 2013. Economic analysis of desalination technologies in the context of carbon pricing, and opportunities for membrane distillation. Desalination **323**:66-74.

López, J., M. Reig, O. Gibert, and J. L. Cortina. 2019. Integration of nanofiltration membranes in recovery options of rare earth elements from acidic mine waters. Journal of Cleaner Production **210**:1249-1260.

Macías, F., R. Pérez-López, M. A. Caraballo, C. R. Cánovas, and J. M. Nieto. 2017. Management strategies and valorization for waste sludge from active treatment of extremely metal-polluted acid mine drainage: A contribution for sustainable mining. Journal of Cleaner Production **141**:1057-1066.

Martínez, N. M., M. D. Basallote, A. Meyer, C. R. Cánovas, F. Macías, and P. Schneider. 2019. Life cycle assessment of a passive remediation system for acid mine drainage: Towards more sustainable mining activity. Journal of Cleaner Production **211**:1100-1111.

Martins, M., E. S. Santos, C. Pires, R. J. Barros, and M. C. Costa. 2010. Production of irrigation water from bioremediation of acid mine drainage: comparing the performance of two representative systems. Journal of Cleaner Production **18**:248-253.

Masindi, V., G. Madzivire, and M. Tekere. 2018. Reclamation of water and the synthesis of gypsum and limestone from acid mine drainage treatment process using a combination of pre-treated magnesite nanosheets, lime, and CO2 bubbling. Water Resources and Industry **20**:1-14.

Mezher, T., H. Fath, Z. Abbas, and A. Khaled. 2011. Techno-economic assessment and environmental impacts of desalination technologies. Desalination **266**:263-273.

Micari, M., A. Cipollina, A. Tamburini, M. Moser, V. Bertsch, and G. Micale. 2019a. Combined membrane and thermal desalination processes for the treatment of ion exchange resins spent brine. Applied Energy **254**.

Micari, M., M. Moser, A. Cipollina, B. Fuchs, B. Ortega-Delgado, A. Tamburini, and G. Micale. 2019b. Techno-economic assessment of multi-effect distillation process for the treatment and recycling of ion exchange resin spent brines. Desalination **456**:38-52.

Micari, M., M. Moser, A. Cipollina, A. Tamburini, G. Micale, and V. Bertsch. 2020. Towards the Implementation of Circular Economy in the Water Softening Industry: A Technical, Economic and Environmental Analysis. Journal of Cleaner Production:Accepted with revisions.

Motsi, T., N. A. Rowson, and M. J. H. Simmons. 2009. Adsorption of heavy metals from acid mine drainage by natural zeolite. International Journal of Mineral Processing **92**:42-48.

Nleya, Y., G. S. Simate, and S. Ndlovu. 2016. Sustainability assessment of the recovery and utilisation of acid from acid mine drainage. Journal of Cleaner Production **113**:17-27.

Papapetrou, M., A. Cipollina, U. La Commare, G. Micale, G. Zaragoza, and G. Kosmadakis. 2017. Assessment of methodologies and data used to calculate desalination costs. Desalination **419**:8-19.

Qin, J., X. Cui, H. Yan, W. Lu, and C. Lin. 2019. Active treatment of acidic mine water to minimize environmental impacts in a densely populated downstream area. Journal of Cleaner Production **210**:309-316.

Sivakumar, M., M. Ramezanianpour, and G. O'Halloran. 2013. Mine Water Treatment Using a Vacuum Membrane Distillation System. APCBEE Procedia **5**:157-162.

Tarutis, W. J. J., L. R. Stark, and F. M. Williams. 1999. Sizing and performance estimation of coal mine drainage wetlands. Ecological Engineering **12**:353-372.

Tiwary, R. K. 2001. Environmental impact of coal mining on water regime and its management. Water, Air and Soil Pollution **132**:185-199.

Turek, M., P. Dydo, and R. Klimek. 2005a. Salt production from coal-mine brine in ED–evaporation–crystallization system. Desalination **184**:439-446.

Turek, M., P. Dydo, and R. Klimek. 2008. Salt production from coal-mine brine in NF — evaporation — crystallization system. Desalination **221**:238-243.

Turek, M., P. Dydo, and A. Surma. 2005b. Zero discharge utilization of saline waters from "Wesola" coal-mine. Desalination **185**:275-280.

Turek, M., K. Mitko, E. Laskowska, M. Chorążewska, K. Piotrowski, A. Jakóbik-Kolon, and P. Dydo. 2018. Energy Consumption and Gypsum Scaling Assessment in a Hybrid Nanofiltration-Reverse Osmosis-Electrodialysis system. Chemical Engineering & Technology **41**:392-400.

Turton, R., R. C. Bailie, W. B. Whiting, J. A. Shaeiwity, and D. Bhattacharzza. 2012. Analysis, Synthesis and Design of Chemical Processes. Prentice Hall.

U.S. Department of the Interior. 2017. Mineral Commodity Summaries - U.S. Geological Survey.

Vince, F., F. Marechal, E. Aoustin, and P. Bréant. 2008. Multi-objective optimization of RO desalination plants. Desalination **222**:96-118.

Wilf, M. 2007. The Guidebook to Membrane Desalination Technology. Balaban Desalination Publications.